

SN 2006AJ ASSOCIATED WITH XRF 060218 AT LATE PHASES:
NUCLEOSYNTHESIS-SIGNATURE OF A NEUTRON STAR-DRIVEN EXPLOSION¹K. MAEDA², K. KAWABATA³, M. TANAKA⁴, K. NOMOTO^{4,5}, N. TOMINAGA⁴, T. HATTORI⁶, T. MINEZAKI⁷, T. KURODA⁴, T. SUZUKI⁴, J. DENG^{8,4,5}, P.A. MAZZALI^{4,5,9,10}, E. PIAN¹⁰*Accepted for publication in the Astrophysical Journal Letters (2007 March 20 issue)*

ABSTRACT

Optical spectroscopy and photometry of SN 2006aj have been performed with the Subaru telescope at $t > 200$ days after GRB060218, the X-ray Flash with which it was associated. Strong nebular emission-lines with an expansion velocity of $v \sim 7,300 \text{ km s}^{-1}$ were detected. The peaked but relatively broad $[\text{OI}] \lambda \lambda 6300, 6363$ suggests the existence of $\sim 2M_{\odot}$ of materials in which $\sim 1.3M_{\odot}$ is oxygen. The core might be produced by a mildly asymmetric explosion. The spectra are unique among SNe Ic in (1) the absence of $[\text{CaII}] \lambda \lambda 7291, 7324$ emission, and (2) a strong emission feature at $\sim 7400 \text{ \AA}$, which requires $\sim 0.05M_{\odot}$ of newly-synthesized ^{58}Ni . Such a large amount of stable neutron-rich Ni strongly indicates the formation of a neutron star. The progenitor and the explosion energy are constrained to $18M_{\odot} \lesssim M_{\text{ms}} \lesssim 22M_{\odot}$ and $E \sim (1-3) \times 10^{51} \text{ erg}$, respectively.

Subject headings: gamma-rays: bursts – supernovae: general – supernovae: individual (SN 2006aj) – nuclear reactions, nucleosynthesis, abundances

1. INTRODUCTION

The connection between long soft Gamma-Ray Bursts (GRBs) and Type Ic Supernovae (SNe Ic) has been observationally established (see Woosley & Bloom 2006 and references therein). It has been argued that well examined GRB-associated SNe (GRB-SNe) are very energetic explosions, called hypernovae, resulting from a massive stellar death. The kinetic energy (E_K) is $E_{51} \equiv E_K/10^{51} \text{ erg s}^{-1} \gtrsim 10$, and the main-sequence mass of the progenitor is $M_{\text{ms}} \sim 40M_{\odot}$ (e.g., SN 1998bw: Iwamoto et al. 1998).

Recently, a new connection between the X-Ray Flash (XRF), which is a low energy analog of a GRB, and an SN Ic has been found. In association with XRF 060218 (Campana et al. 2006), SN Ic 2006aj was discovered (Ferrero et al. 2006; Mirabal et al. 2006; Modjaz et al. 2006; Pian et al. 2006; Soderberg et al. 2006; Sollerman et al. 2006).

At early phase, SN 2006aj showed velocities intermediate between GRB-SNe and canonical SNe Ic. The $[\text{OI}] \lambda 7774$ absorption was weak. The light curve evolved

¹ Based on data collected at Subaru Telescope, which is operated by the National Astronomical Observatory of Japan.

² Department of Earth Science and Astronomy, Graduate School of Arts and Science, University of Tokyo, 3-8-1 Komaba, Meguro-ku, Tokyo 153-8902, Japan: maeda@esa.c.u-tokyo.ac.jp

³ Hiroshima Astrophysical Science Center, Hiroshima University, Hiroshima 739-8526, Japan

⁴ Department of Astronomy, School of Science, University of Tokyo, Bunkyo-ku, Tokyo 113-0033, Japan

⁵ Research Center for the Early Universe, School of Science, University of Tokyo, Bunkyo-ku, Tokyo 113-0033, Japan

⁶ Subaru Telescope, National Astronomical Observatory of Japan, Hilo, HI 96720, USA

⁷ Institute of Astronomy, School of Science, University of Tokyo, 2-21-1 Osawa, Mitaka, Tokyo 181-0015, Japan

⁸ National Astronomical Observatories, CAS, 20A Datun Road, Chaoyang District, Beijing 100012, China

⁹ Max-Planck-Institut für Astrophysik, Karl-Schwarzschild-Straße 1, 85741 Garching, Germany

¹⁰ National Institute for Astrophysics–OATs, Via G.B. Tiepolo 11, 34143 Trieste, Italy

more quickly than other GRB-SNe. Mazzali et al. (2006) concluded that SN 2006aj is less energetic ($E_{51} \sim 2$) than other GRB-SNe and ejected a smaller amount of ^{56}Ni [$M(^{56}\text{Ni}) \sim 0.2M_{\odot}$]. They suggested that the main-sequence mass of the progenitor is $M_{\text{ms}} \sim 20 - 25M_{\odot}$, and hence that XRF-associated SN 2006aj was driven by a neutron star (NS) formation.

In this *Letter*, we present observations of SN Ic 2006aj at $t \gtrsim 200$ days with the Subaru telescope (hereafter t is the rest frame time since 2006 February 18). We show that the nebular phase data provide constraints on nucleosynthesis and the compact remnant.

2. OBSERVATIONS AND DATA REDUCTION

We performed spectroscopic and photometric observations of SN 2006aj on 2006 September 17 (UT: $t = 204$ days) and November 27 (273 days) with the 8.2 m Subaru telescope equipped with the Faint Object Camera and Spectrograph (FOCAS: Kashikawa et al. 2002). For spectroscopy, we used 0''.8 width slit and the B300 grism, which gave a wavelength coverage of 4700–9000 Å and a spectral resolution of $\simeq 10.7 \text{ \AA}$. The exposure times were 2,800 s and 5,400 s, respectively. For flux calibration, GD71 and BD +28°4211 were observed.

For photometry, we obtained B - (60 s), V - (60 s) and R -band (60 s) images in September and B - (300 s), V - (180 s), and R -band (180 s) images in November. We obtained images of standard stars around PG0220+132 and SA98-634 for photometric calibrations. Our photometry is shown in Table 1 and the photometry-calibrated spectra in Figure 1.

The spectra are the sum of the SN and host galaxy spectra (Fig. 1). We find broad emission lines with the corresponding expansion velocity $v \sim 7,300 \text{ km s}^{-1}$ at both epochs (Fig. 2: see also Foley et al. 2006). Especially strong is $[\text{OI}] \lambda \lambda 6300, 6363$. So the existence of a SN Ic in XRF 060218 is unambiguously confirmed.

The continuum level is almost identical in both epochs. Since no strong emission from an SN is expected at $\sim 6100, 6800$, and 8000 Å, we regard the flux level of the

continuum connecting these wavelengths to be the host contribution, expressed as $-2.0 \times 10^{-17} \times (\lambda/6000\text{\AA}) + 4.1 \times 10^{-17} \text{ erg s}^{-1} \text{ cm}^{-2} \text{ \AA}^{-1}$ (Fig. 1). The derived host magnitude is fainter than that estimated by Sollerman et al. (2006) by about 0.3 mag in V - and R -bands, while the color $V - R$ is consistent. The difference probably stems from the systematic errors. The host is blue, as expected from its faintness and low metallicity (Sollerman et al. 2006).

3. ANALYSES OF SPECTRUM FEATURES

Figure 2 shows that the nebular spectra of SN 2006aj have the following two unique features compared with other SNe Ic. (1) $[\text{CaII}]\lambda\lambda 7291, 7324$ is absent. (2) A strong emission feature is seen at $\sim 7,400\text{\AA}$. In this *Letter*, we adopt $\mu = 35.84$ and $E(B - V) = 0.13$ (Pian et al. 2006). Our discussion is based on the September spectrum.

3.1. Total Mass at $v \lesssim 7,300 \text{ km s}^{-1}$

The bolometric luminosity (L_{bol}) is expressed as (e.g., Maeda et al. 2003a),

$$L_{\text{bol}} = (D_{\gamma} + 0.035)L_{\gamma}, \quad (1)$$

at a nebular epoch. Here the γ -ray energy input rate from $M^{(56)\text{Ni}} = 0.2M_{\odot}$ is $L_{\gamma} = 4.4 \times 10^{41} \text{ erg s}^{-1}$ at $t \sim 204$ days. D_{γ} ($\sim 3\tau_{\gamma}/4$ for a homogeneous nebula, which is a good approximation at low velocities) is the fraction of the γ -ray energy deposited within the SN nebula, and 0.035 accounts for the *in situ* positron deposition rate. The optical depth to the γ -rays is

$$\tau_{\gamma} = 0.071 \left(\frac{M_{7300}}{M_{\odot}} \right) \left(\frac{v}{7,300 \text{ km s}^{-1}} \right)^{-2} \left(\frac{t}{204 \text{ days}} \right)^{-2}, \quad (2)$$

where M_{7300} denotes the total mass ejected with $v \lesssim 7,300 \text{ km s}^{-1}$. Substituting $L_{\text{bol}} \sim 6.2 \times 10^{40} \text{ erg s}^{-1}$ (taking into account the reddening and a typical NIR contribution $\sim 20\%$; Tomita et al. 2006) into equations (1) and (2), we obtain $M_{7300} \sim 2M_{\odot}$.

3.2. Absence of Ca Lines and Ejecta Structure

No detection of $[\text{CaII}]$ and CaII IR triplet provides the following constraints. In a core-collapse SN explosion, more than $4 \times 10^{-3}M_{\odot}$ of Ca is synthesized if $E_{51} \gtrsim 1$ (e.g., Nakamura et al. 2001). In an SN Ic, the emissivity of $[\text{CaII}]\lambda\lambda 7291, 7324$ is about three orders of magnitudes larger than $[\text{OI}]\lambda\lambda 6300, 6363$. If Ca co-existed with O, Ca^+ would be the predominant ion (e.g., Fransson & Chevalier 1989). Thus, if Ca ($\gtrsim 4 \times 10^{-3}M_{\odot}$) and O were *microscopically* mixed, then M_{O} would have been much larger than $20M_{\odot}$ to satisfy the observed upper limit for the $[\text{CaII}]$ (Fig. 2). This is inconsistent with $M_{7300} \sim 2M_{\odot}$ (§3.1).

The separation of Ca and O occurs naturally in ordinary supernova models. This is also seen in *Spitzer* observations of Cas A (Ennis et al. 2006). Nucleosynthesis calculations show that the explosion produces chemically distinct regions: Fe-rich materials (where ^{56}Ni is the predominant product), Si-rich materials (where most of Ca is produced), and O-rich materials (mostly O and some unburned C). These regions may well be mixed

macroscopically in velocity space (e.g., by jets: Maeda & Nomoto 2003b; Maeda 2006b), but not *microscopically*. Hereafter, $M_{\text{Fe-rich}}$, $M_{\text{Si-rich}}$, and $M_{\text{O-rich}}$, respectively, denote the masses of the Fe-rich, Si-rich, and O-rich materials ejected with $v \lesssim 7,300 \text{ km s}^{-1}$.

In this "microscopically separated" model, the sum of the $[\text{CaII}]$ and CaII luminosities (L_{CaII}) is related to the mass of the Si-rich region rather than the mass of Ca itself, i.e.,

$$L_{\text{CaII}} \sim L_{\gamma} X_{\text{Si-rich}} D_{\gamma} \alpha_{\text{Si}} f_{\text{CaII}}, \quad (3)$$

where the fraction of the absorbed γ -ray energy going into the Ca lines would be $f_{\text{CaII}} \sim 0.5$, with the remaining fraction mostly going into $[\text{SiII}]$ NIR lines. $X_{\text{Si}} \equiv M_{\text{Si-rich}}/M_{7300}$ is the mass fraction of the Si-rich region. A factor, α_{Si} , accounts for the fact that the γ -rays are scattered more easily within the Fe-rich region than in the other regions, because the γ -rays begin their flight in the Fe-rich region. At late epochs, the mean free path of the γ -rays is larger than the size of the nebula, thus α_{Si} is an order of unity. Taking the upper limit $L_{\text{CaII}} \lesssim 7 \times 10^{39} \text{ erg s}^{-1}$, we obtain

$$M_{\text{Si-rich}} \lesssim 0.6M_{\odot}(1/\alpha_{\text{Si}})(0.5/f_{\text{CaII}}). \quad (4)$$

The upper limit is even tighter according to the spectrum synthesis (§3.5), i.e., $M_{\text{Si-rich}} \lesssim 0.15M_{\odot}$, because other lines (e.g., $[\text{FeII}]$) should also have large contribution.

3.3. Masses of Oxygen and Fe-peak Elements

From the masses we have obtained as $M_{7300} \sim 2M_{\odot}$, $M_{\text{Si-rich}} \lesssim 0.15M_{\odot}$, and $M^{(56)\text{Ni}} \sim 0.2M_{\odot}$, we derive $M_{\text{O-rich}} \sim 1.6M_{\odot}$ and $M_{\text{Fe-rich}} \sim 0.3M_{\odot}$. We here examine if $M_{\text{O-rich}}$ and $M_{\text{Fe-rich}}$ are consistent with the reddening-corrected luminosity of $[\text{OI}]\lambda\lambda 6300, 6363$ (L_{OI}) and that of $[\text{FeII}]$ and $[\text{NiII}]$ ($L_{\text{Fe-peak}}$: integrated in 4700 - 5500 \AA and 7000 - 7600 \AA).

Following the argument similar to the one used in deriving equation (4), we obtain

$$M_{\text{O-rich}} \sim 1.6M_{\odot}(0.7/\alpha_{\text{O}})(0.7/f_{\text{OI}}), \quad (5)$$

with $L_{\text{OI}} \sim 1.7 \times 10^{40} \text{ erg s}^{-1}$. Hereafter, α_{i} and X_{i} (where $\text{i} = \text{Fe, Si and O}$) are used for the Fe-, Si-, and O-rich regions in the same way as α_{Si} and $X_{\text{Si-rich}}$. f_{OI} is the fraction of the absorbed γ -ray energy going into $[\text{OI}]\lambda\lambda 6300, 6363$ (with remaining fraction going into $[\text{CI}]\lambda 8727$ and $[\text{OI}]\lambda 7774$). Equation (5) shows that $\alpha_{\text{O}} \sim 0.7$ is necessary to reproduce L_{OI} . To meet the trivial relations $\sum_{\text{i}} X_{\text{i}} \alpha_{\text{i}} = 1$ and $\sum_{\text{i}} X_{\text{i}} = 1$, $\alpha_{\text{Fe}} \sim 2.6$ is required. With this value, the spectrum synthesis (§3.5) well reproduces $L_{\text{Fe-peak}} \sim 2 \times 10^{40} \text{ ergs s}^{-1}$.

These values for α_{i} are physically reasonable. For an SN nebula having a constant density with $M_{\text{Fe-rich}} = 0.3M_{\odot}$, $M_{\text{Si-rich}} = 0.1M_{\odot}$, and $M_{\text{O-rich}} = 1.6M_{\odot}$, we derive $\alpha_{\text{Fe-rich}} \sim 2.9$, $\alpha_{\text{Si-rich}} \sim 1.8$, and $\alpha_{\text{O-rich}} \sim 0.6$ by our 1D γ -ray transport calculation. These are obtained for a concentric distribution (with the Fe region in the center), but it gives an approximately correct estimate even for a jet/blob-like distribution of the Fe-rich materials.

3.4. $[\text{NiII}]\lambda 7380$ and stable ^{58}Ni

The strong emission at $\sim 7400\text{\AA}$ is not common for SNe Ib/c, although in other SNe Ib/c the feature may be

hidden by the [CaII]. The contribution from [FeII] $\lambda 7388$ and [FeII] $\lambda 7452$ (a^4F - a^2G) should be small. The radiative transition probabilities of the [FeII] are smaller than those of [FeII] $\lambda 7172$ and [FeII] $\lambda 7155$ that arise from the same transitions, and the luminosity at $7100 - 7200\text{\AA}$ is only one-third of the luminosity of the 7400\AA feature.

We suggest that the 7400\AA feature is [NiII] $\lambda 7380$ (Fig. 2), as also seen in the Crab Nebula (MacAlpine et al. 2007). From the spectrum synthesis (§3.5), we find that this feature is reproduced by [NiII] $\lambda 7380$ if the mass of Ni is $\sim 0.05M_\odot$. Since virtually all ^{56}Ni already decayed at $t \gtrsim 200$ days, this must be stable ^{58}Ni .

3.5. Spectrum Synthesis

To confirm the above results, we perform nebular spectrum synthesis calculations. We set the masses at $v \leq 7,300 \text{ km s}^{-1}$ as follows: $M_{\text{O-rich}} = 1.6M_\odot$ (where $M_{\text{O}} = 1.3M_\odot$ and $M_{\text{C}} = 0.3M_\odot$), $M_{\text{Si-rich}} = 0.1M_\odot$ (where $M_{\text{Si}} = 0.08M_\odot$, $M_{\text{S}} = 0.01M_\odot$, $M_{\text{Ca}} = 4 \times 10^{-3}M_\odot$, and $M_{\text{Fe}} = 4 \times 10^{-3}M_\odot$), and $M_{\text{Fe-rich}} = 0.3M_\odot$ [where $M^{(56)\text{Ni}} = 0.2M_\odot$ and $M^{(58)\text{Ni}} = 0.06M_\odot$]. We set $\alpha_{\text{Fe}} = 2.6$, $\alpha_{\text{Ca}} = 1.0$, and $\alpha_{\text{O}} = 0.7$ for the γ -ray deposition (§3.3).

A one-zone spectrum synthesis is applied to the O-rich, Si-rich, and Fe-rich materials. A Monte-Carlo γ -ray transport calculation is performed for a uniform nebula with $M_{7300} = 2M_\odot$, $M^{(56)\text{Ni}} = 0.2M_\odot$. The deposited luminosity is apportioned to each region according to $X_i\alpha_i$ (equation 3). Positrons deposit their energy only to the Fe-rich materials.

With the deposition luminosity, non-LTE rate equations coupled with the ionization-recombination equilibrium are solved for each region (Mazzali et al. 2001). The model spectrum fits the observed one fairly well (Fig. 3). The feature at $\sim 7,400\text{\AA}$ is well explained by [NiII] $\lambda 7380$ (§3.3) from $\sim 0.05M_\odot$ of stable Ni.

4. PROPERTIES OF THE PROGENITOR AND ITS EXPLOSION

We have derived the masses as follows (§3): $M_{7300} \sim 2M_\odot$, $M_{\text{O-rich}} \sim 1.6M_\odot$ (i.e., $M_{\text{O}} \sim 1.3M_\odot$ if 80% is oxygen), $M_{\text{Si-rich}} \lesssim 0.15M_\odot$, and $M_{\text{Fe-rich}} \sim 0.3M_\odot$ (where $M^{(56)\text{Ni}} \sim 0.2M_\odot$ and $M^{(58)\text{Ni}} \sim 0.05M_\odot$).

Progenitor Mass: The masses of $M_{\text{O}} \sim 1.3M_\odot$ and $M_{7300} \sim 2M_\odot$ provide strong constraints on M_{ms} as follows. Theoretical models show $M_{\text{O}} < 1.3M_\odot$ in the whole ejecta if $M_{\text{ms}} \lesssim 18M_\odot$ (Nomoto & Hashimoto 1988). This leads to the lower limit of $M_{\text{ms}} \gtrsim 18M_\odot$.

For given E_{51} , larger M_{ms} results in larger M_{7300} . Our spherical calculations show $M_{7300} > 2M_\odot$ if $M_{\text{ms}} \gtrsim 22M_\odot$ and $E_{51} = 2$. Since explosion asymmetry only increases the mass at the low velocity (Maeda et al. 2002; Maeda & Nomoto 2003b), the result of the spherical calculations can be used to place the upper limit to M_{ms} . We thus obtain $M_{\text{ms}} \lesssim 22M_\odot$. Therefore, we narrow down the progenitor mass range as $18M_\odot \lesssim M_{\text{ms}} \lesssim 22M_\odot$.

The total oxygen mass is $\sim 2.3M_\odot$ in the ejecta, since the oxygen mass at $v \gtrsim 7,300 \text{ km s}^{-1}$ is $\sim 1M_\odot$ (Mazzali et al. 2006). This is consistent with $M_{\text{ms}} \sim 22M_\odot$.

Explosion Energy: $M_{\text{Si-rich}} \lesssim 0.15M_\odot$ (§3.2) gives information on E_{51} . The mass of the Si-rich region is

larger for larger M_{ms} (because of the higher progenitor density) and for larger E_{51} (because of the more extended burning). According to our explosion models (e.g., Nakamura et al. 2001), we obtain the constraints of $M_{\text{ms}} \lesssim 25M_\odot$ and $E_{51} \lesssim 3$.

NS Formation: $M^{(58)\text{Ni}} \sim 0.05M_\odot$ provides a strong indication of the NS formation. The large amount of ^{58}Ni indicates that neutron-rich materials are ejected from the vicinity of the central remnant. Our models for $M_{\text{ms}} = 20M_\odot$ and $E_{51} \sim 2.5$ shows that $M^{(56)\text{Ni}} \sim 0.2M_\odot$ and $M^{(58)\text{Ni}} \sim 0.04M_\odot$ if the remnant's mass is $M_{\text{cut}} \sim 1.4M_\odot$. If $M_{\text{cut}} \sim 1.5M_\odot$, then $M^{(56)\text{Ni}} \sim 0.16M_\odot$ and $M^{(58)\text{Ni}} \sim 9 \times 10^{-4}M_\odot$. For $M_{\text{cut}} \sim 1.6M_\odot$, $M^{(56)\text{Ni}} \sim 0.07M_\odot$ and $M^{(58)\text{Ni}} \sim 3 \times 10^{-4}M_\odot$. The NS formation is also consistent with $M^{(56)\text{Ni}} \sim 0.2M_\odot$.

5. DISCUSSION

5.1. Signatures of an Asymmetric Explosion

In GRB-SN 1998bw, the observed mass at low velocities exceeds that predicted by the spherical explosion model, which suggests that the explosion is aspherical (Mazzali et al. 2001; Maeda et al. 2003a, 2006ac). On the other hand, the existence of the asymmetry is not clear in SN 2006aj. $M_{7300} \sim 2M_\odot$ (§3) is consistent with the spherical explosion model for a CO star with $M_{\text{ms}} \sim 22M_\odot$ and $E_{51} \sim 2$.

We note, however, that the spherical model has a low density hole at $v \lesssim 2,000 - 2,500 \text{ km s}^{-1}$. The mildly-peaked [OI] $\lambda\lambda 6300, 6363$ profile shows an enhancement of the material density at $v \lesssim 3,000 \text{ km s}^{-1}$. This indicates an asymmetric explosion, as also suggested by polarizations (Gorosabel, et al. 2006). The asymmetry might be produced either by a jet-like explosion or Rayleigh-Taylor instability at the Si/CO interface (Kifonidis et al. 2003). If this is a signature of a jet-like aspherical SN explosion, the jet would be wider than in SN 1998bw (intrinsically or due to stronger lateral expansion; Maeda & Nomoto 2003b), since the signature is seen only in the innermost part (see also Mazzali et al. 2007).

5.2. Relations to other SNe Ib/c and SN 1998bw

The absence of [CaII] $\lambda\lambda 7291, 7324$ indicates that the chemically distinct regions are not microscopically mixed to one another (§3.2). This is probably the case in SNe Ib/c in general: otherwise the [CaII] would be much stronger than [OI] $\lambda\lambda 6300, 6363$ in most SNe Ib/c, as is contrary to observations (e.g., Matheson et al. 2001).

Why the [CaII] is absent only in SN 2006aj may be answered from a tendency of E_{51} as a function of M_{ms} . For progenitors with $M_{\text{ms}} \lesssim 20M_\odot$, the [CaII] can be strong relative to the [OI], because $M_{\text{O-rich}}$ is smaller than in SN 2006aj despite similar $M_{\text{Si-rich}}$ (since $E_{51} \sim 1 - 2$). For hypernovae with $M_{\text{ms}} \sim 40M_\odot$ (e.g., SN 1998bw), the [CaII] can be strong since the large $E_{51} \gtrsim 10$ yields large $M_{\text{Si-rich}}$. Thus, presence of the [CaII] in the majority of normal SNe Ib/c suggests that such normal SNe Ib/c may have originated in relatively low-mass stars with $M_{\text{ms}} \lesssim 20M_\odot$. This implies that they evolve through binary paths, since single stars with this mass range are expected to end as SNe II (Hirschi et al. 2005).

supported by NSFC grant 10673014.

REFERENCES

- Campana, S., et al. 2006, *Nature*, 442, 1008
 Ennis, J.A., et al. 2006, *ApJ*, 652, 376
 Ferrero, P., et al. 2006, *A&A*, 457, 857
 Foley, R.J., Bloom, J.S., Perley, D.A., & Butler, N.R. 2006, *GCN Circ.* 5376
 Fransson, C., & Chevalier, R.A. 1989, *ApJ*, 343, 323
 Gorosabel, J., et al. 2006, *A&A*, 459, L33
 Hirschi, R., Meynet, G., & Maeder, A. 2005, *A&A*, 433, 1013
 Iwamoto, K., et al. 1998, *Nature*, 395, 672
 Kashikawa, N., et al. 2002, *PASJ*, 54, 819
 Kifonidis, K., Plewa, T., Janka, H.-Th., & Müller, E. 2003, *A&A*, 408, 621
 MacAlpine, G.M., et al. 2007, *AJ*, 133, 81
 Maeda, K., et al. 2002, *ApJ*, 565, 405
 Maeda, K., et al. 2003a, *ApJ*, 593, 931
 Maeda, K., & Nomoto, K., 2003b, *ApJ*, 598, 1163
 Maeda, K., Nomoto, K., Mazzali, P.A., & Deng, J. 2006a, *ApJ*, 640, 854
 Maeda, K. 2006b, *ApJ*, 644, 385
 Maeda, K., Mazzali, P.A., & Nomoto, K. 2006c, *ApJ*, 645, 1331
 Matheson, T., Filippenko, A.V., Leonard, D.C., & Shields, J.C. 2001, *AJ*, 121, 1648
 Mazzali, P.A., Nomoto, K., Maeda, K., & Patat, F. 2001, *ApJ*, 559, 1047
 Mazzali, P.A., et al. 2006, *Nature*, 442, 1018
 Mazzali, P.A., et al. 2007, *ApJ*, in press
 Mirabal, N., Halpern, J.P., An, D., Thorstensen, J.R., & Terndrup, D.M., 2006, *ApJ*, 643, L99
 Modjaz, M., et al. 2006, *ApJ*, 645, L21
 Nakamura, T., et al. 2001, *ApJ*, 555, 880
 Nomoto, K., & Hashimoto, M. 1988, *Phys. Rep.*, 163, 13
 Pian, E., et al. 2006, *Nature*, 442, 1011
 Soderberg, A.M., et al. 2006, *Nature*, 442, 1014
 Sollerman, J., et al. 2006, *A&A*, 454, 503
 Tomita, H., et al. 2006, *ApJ*, 644, 400
 Woosley, S.E., & Bloom, J.S. 2006, *ARA&A*, 44, 507

TABLE 1
PHOTOMETRY

Date/Component	<i>B</i>	<i>V</i>	<i>R</i>
September 17 ^a	20.64 ± 0.1	20.23 ± 0.1	19.82 ± 0.1
November 27 ^a	20.71 ± 0.1	20.34 ± 0.1	19.86 ± 0.1
Host (Subaru) ^b	...	20.53	20.16
SN on September ^c	...	22.45	21.74
SN on November ^c	...	22.94	22.21
Host (Sollerman) ^d	20.46 ± 0.07	20.19 ± 0.04	19.86 ± 0.03

^aUsing the FOCAS filter system, which is similar to the Johnson-Cousins system (Kashikawa et al. 2002).

^bSee §2 and Figure 1 for the assumed host spectrum. The photometry is given for the Johnson-Cousins system.

^cThe intrinsic SN magnitude obtained after subtracting the host contribution and removing narrow emission lines. In the Johnson-Cousins system.

^dThe host magnitude estimated by Sollerman et al. (2006)

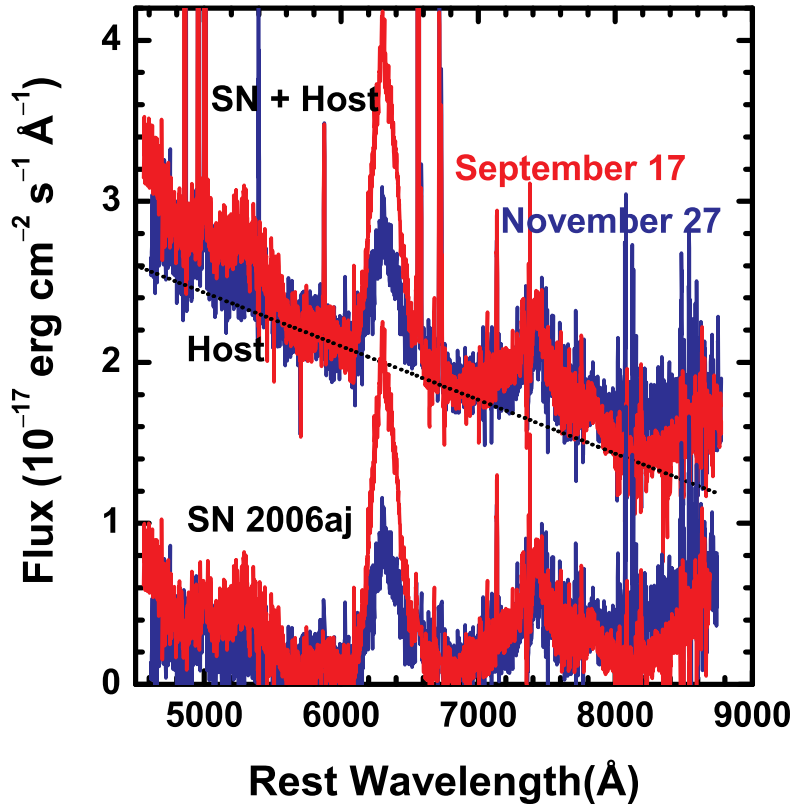


FIG. 1.— Reduced spectra of SN 2006aj on 2006 September 17 (red), and on 2006 November 27 (blue). The flux is calibrated with the photometry. The redshift of the host ($z = 0.0335$) is corrected for. The assumed host galaxy contribution (§2) is shown by the black dotted line. The intrinsic SN spectra, after subtracting the host contribution and removing major narrow emission lines, are also shown (bottom).

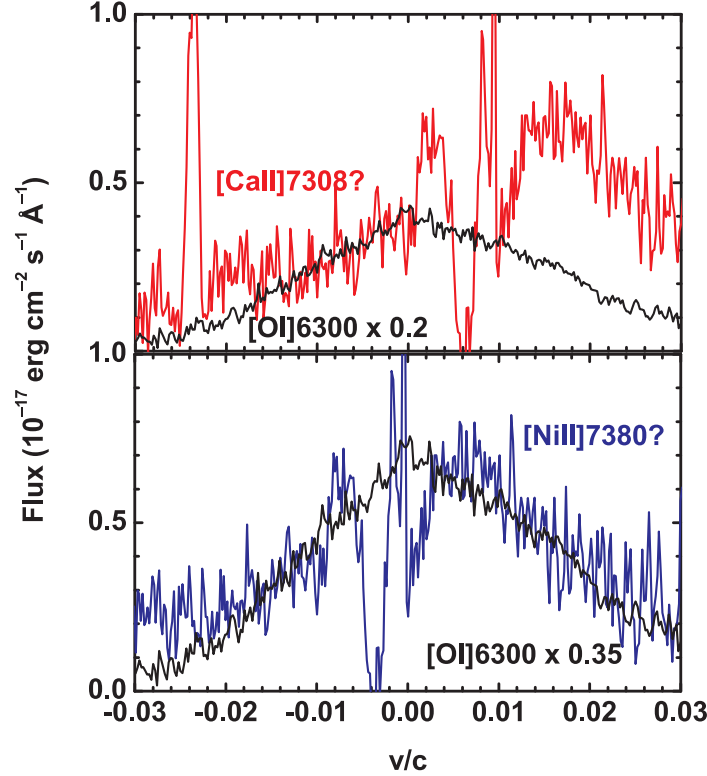


FIG. 2.— Comparison of emission profiles. (a) Comparison of $[\text{OI}]\lambda\lambda 6300, 6363$ (black) with $[\text{CaII}]\lambda\lambda 7291, 7324$ (red). The center of the wavelength is assumed to be 6300 and 7308Å for the [OI] and [CaII], respectively. (b) Comparison of the [OI] (black) with the emission feature centered at 7380Å(blue). We suggest that the feature is $[\text{NiII}]\lambda 7380$. Note that an atmospheric absorption at $\sim 7,400\text{\AA}$ is not removed.

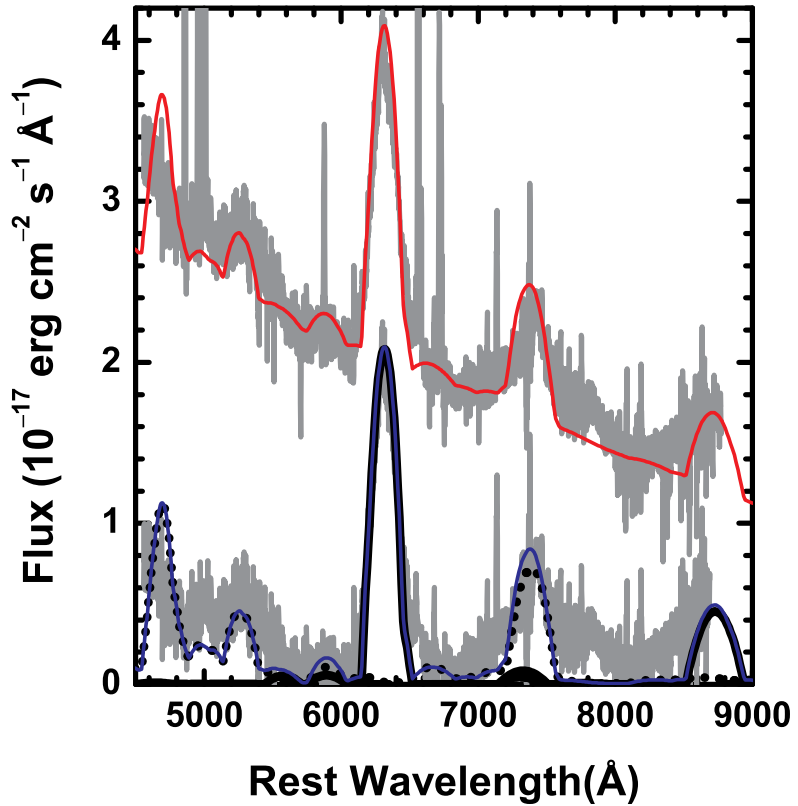


FIG. 3.— Synthetic spectrum as compared with the September spectrum. The model spectrum, reddened with $E(B - V) = 0.13$, is compared with the host-subtracted SN spectrum at the SN rest frame (blue). For presentation, the fit to the original spectrum is also shown (red), in which the host spectrum (Fig. 1) is added to the model spectrum. For the model spectrum, the individual contributions from the O-rich (black solid), Si-rich (dashed), and Fe-rich (dotted) regions are shown.